

Visual Localization Using Semantic Segmentation and Depth Prediction

Huanhuan Fan* Yuhao Zhou* Ang Li† Shuang Gao Jijunnan Li Yandong Guo
OPPO Research Institute

{zhouyuhao, fanhuanhuan, liang, gaoshuang, lijijunnan, guoyandong}@oppo.com

Abstract

In this paper, we propose a monocular visual localization pipeline leveraging semantic and depth cues. We apply semantic consistency evaluation to rank the image retrieval results and a practical clustering technique to reject estimation outliers. In addition, we demonstrate a substantial performance boost achieved with a combination of multiple feature extractors. Furthermore, by using depth prediction with a deep neural network, we show that a significant amount of falsely matched keypoints are identified and eliminated. The proposed pipeline outperforms most of the existing approaches at the Long-Term Visual Localization benchmark 2020¹.

1. Introduction

Visual localization is one of the major challenges and the fundamental capability for numerous computer vision applications, such as augmented reality, intelligent robotics, or long-term visual navigation of autonomous driving[1][2]. A core task for these applications is to find the precise location of any query image with a map of 3-dimensional (3D) points reconstructed by structure-from-motion (SfM) with database images[3][4][5]. The map is typically used to describe the position of landmarks[6][7], i.e., 3D points and structures in the environments, which are pre-collected from the point features extracted from the database images. Every point feature is associated with a 3D position in the world coordinates and a unique descriptor of its visual appearance. During localization, the points in the 2D query image and the points with 3D world coordinates in the map is determined, and finally the 6-Degree-of-Freedom (DoF) pose of query image is recovered with Perspective-n-Point (PnP)[8].

There are several critical challenges associated with the repeatability of traditional feature descriptors including SIFT[9] and BRIEF[7], which are shown to

be highly sensitive to large variation in viewpoint and illumination[10][11][12][13]. Consequently, localization pipelines struggle to find enough 2D-3D matched pairs to facilitate the successful 6DoF pose estimation. In addition, our experimental results show that keypoints are often incorrectly matched even after a standard RANSAC-based outlier rejection mechanism[14].

In this paper, we propose the following key enhancement on the retrieval-based visual localization pipeline to handle the problems. **(i)** We evaluate the confidence of every image retrieval result with the proposed *semantic consistency weight* (SCW), which ranks the retrieved results based on the ratio of matched keypoints with consistent semantic label. **(ii)** The outliers of pose estimates are identified by a practical clustering technique. **(iii)** We demonstrate the effectiveness of jointly using multiple learning-based features and descriptors for improved 6DoF pose estimation. **(iv)** The enhanced R2D2 descriptor enables higher matching accuracy. **(v)** False keypoint matching relations are identified with the proposed *semantic consistency check* (SCC) and *depth consistency verification* (DCV) procedure. **(vi)** We leverage semantic segmentation with the proposed weighted-RANSAC scheme that adaptively adjusts the RANSAC threshold.

2. Method

2.1. Overview

Long-term visual localization is a challenging task due to weak textures and potentially huge variation in viewpoint and illumination. Figure 1 illustrates the proposed localization pipeline based on a standard retrieval-based framework in[15], which consists of three main modules as follows.

(i) Map construction. With database images captured at the target scene, we first run a standard SfM algorithm to construct a 3D model, represented by a large number of 3D interest points. At the same time, the 2D-3D keypoint matching relations produced during SfM are recorded for run-time pose estimation. Moreover, semantic segmentation is estimated for every database image and semantic labels are associated with the 3d points.

*Equal contribution.

†Corresponding author.

¹<https://www.visuallocalization.net/>

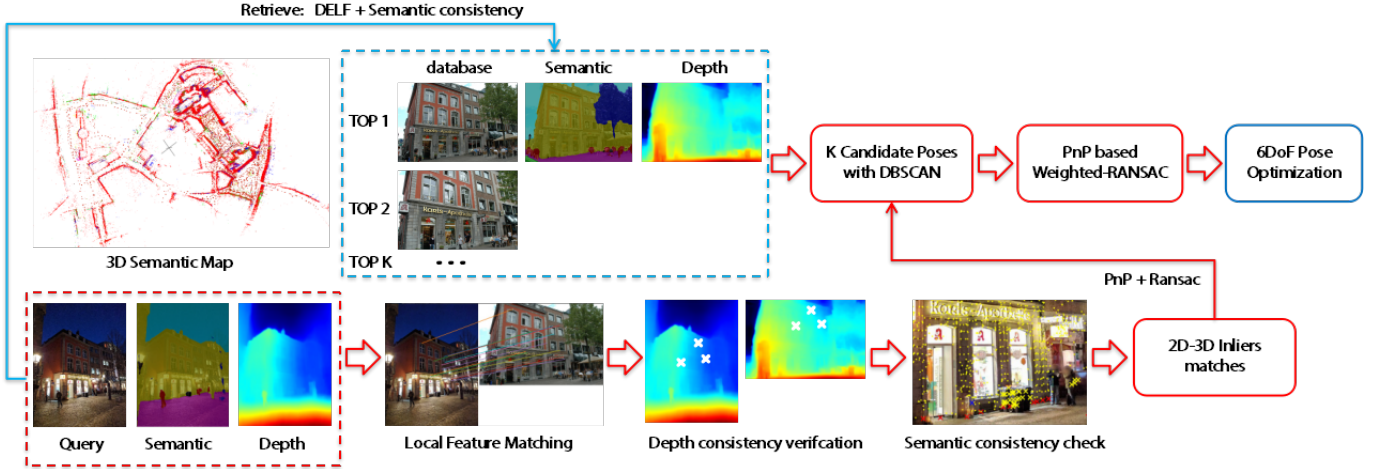


Figure 1: An overview diagram of the proposed pipeline.

(ii) **Image retrieval.** A coarse search is performed by matching the query with the database images using global descriptors computed by a deep neural network reported in [16]. Though this process is efficient given that there are far fewer database images than the 3D points in SfM model, it often produces incorrect results, especially under large variation of viewpoint and illumination. We handle this problem by first calculating homography matrices with existing matched pairs, and cluster the results to reject outliers that correspond to incorrect retrieval results. Furthermore, we propose SCW, which reranks the retrieval results with a verification step considering semantic consistency. As a result, a number of candidate images are discovered that are semantically consistent to the query image.

(iii) **Feature matching and pose estimation.** 2D interest points are extracted from query and matched against keypoints in every candidate image, 2D-3D query-database matching relations are built for PnP pose estimation. Nevertheless, our experimental results show that incorrect matches are often produced despite of the RANSAC mechanism. This issue is handled by the following sub-modules. Firstly, a combination of multiple learning-based feature extractors is used which produces substantially more feature points. Secondly, SCC and DCV are performed for semantic and depth consistency verification, which essentially remove weakly consistent matches. Finally, all matching relations are weighted with consistency scores for bias sampling during the novel weighted-RANSAC and PnP.

2.2. Semantic verification of image retrieval

Recently, learning-based approaches achieve impressive performance on image retrieval[17][18][16][19][20]. Our experimental results show that DEep Local Feature (DELf)[16] produces the best results. Therefore, we apply DELf to obtain a predefined number of candidate images.

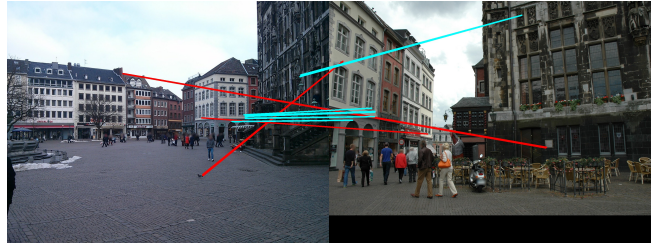


Figure 2: Experiment results on SCC: matching results of KNN+RANSAC in red and KNN+SCC+RANSAC in cyan.

Nevertheless, a significant amount incorrect results are inevitably generated. This problem is handled by the proposed SCW and a clustering approaches. Current state-of-the-art semantic segmentation approaches are mainly based on deep neural networks, such as PSPNET[21], BiSeNet[22] and DeepLabv3+[23], where DeepLabv3+ is selected for our pipeline that attains superior performance on PASCAL VOC2012[24] and Cityscapes[25]. For every retrieved image, the homography matrix from the query image is computed by RANSAC, producing a number of inliers, denoted by S_c . We also count the number of matches with identical semantic label represented by S_f . SCW is then defined by

$$S_R = \frac{\alpha_1 S_c + \alpha_2 S_f}{\alpha_1 + \alpha_2}, \quad (1)$$

where α_1 and α_2 are scalars associated with scoring weights. SCW is then calculated for all query-retrieval pairs, and only those with high SCW scores will proceed to subsequent steps. Due to inaccurate semantic prediction, a number of incorrect candidate images may still present. This issue is tackled with a standard clustering technique that effectively rules out the outliers of pose estimates produced by the problematic retrieval results.

Semantic consistency is also computed to eliminate the inconsistent matches with the proposed SCC, described as follows. For an output matched pair of features, the semantic labels of both query point and retrieved point are compared, and pairs with different labels are considered as unsuccessful and thus discarded. In addition, features points on dynamic objects including pedestrians and vehicles are also removed. Figure 2 shows a comparison of the matching results before and after introducing SCC, where incorrect matches are eliminated. Note that SCC is applied before RANSAC.

2.3. Multiple feature extractors and enhanced R2D2 descriptor

Recently, learning based feature extractors and descriptors are shown to outperform traditional handcrafted ones including SIFT [26] [27] [28]. Learning-based feature extractors are trained on large datasets and are able to automatically discover feature extraction process and representation most suited to the data. SuperPoint[11] and R2D2[10] are amongst the most recent approaches that achieve impressive performance. While SuperPoint[11] is trained to extract multi-scale SIFT-like salient features, R2D2[10] focuses on extracting discriminant features with low repeatability, i.e. avoid repeating features such as windows. Our experimental results show that a simple combination of features by both detectors results in a significant increase in the number of matched pairs, which in turn leads to higher pose estimation accuracy.

Furthermore, an in-depth study on the R2D2 algorithm shows that the confidence of a matching result is closely related to the similarity between the descriptor score of the two features. In other words, a pair of matched keypoints with similar descriptor score is more likely to be true than ones with very different score. Thus, the proposed modification on R2D2 descriptor involves incorporating the detection confidence score by

$$d' = d \times s, \tag{2}$$

where d is the original descriptor, s is the descriptor score and d' is the new descriptor with proposed modification.

In order to allow realistic and reliable comparisons in different environments, we tested the modified R2D2 descriptor on the HPatches dataset[29], the one of the most recent ones for evaluation of different feature descriptors. The performance of the proposed modification is evaluated with the mean matching accuracy (MMA), and compared with other latest descriptors including the original R2D2, DELF[16], HardNet++ descriptors with HesAffNet regions[27][30] (HAN + HN++), SuperPoint[11], D2-Net[31] and a handcrafted Hessian affine detector with RootSIFT descriptor[32]. Figure 3 shows the results for illumination and viewpoint changes, as well as the overall

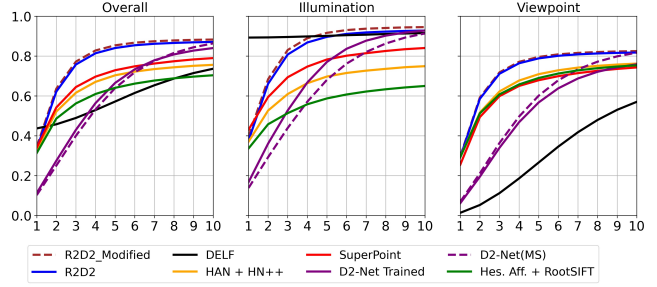


Figure 3: Comparison with the original R2D2 descriptor and other state of the art using the MMA (vertical axis) for varying reprojection error thresholds (horizontal axis, in pixel) on the HPatches dataset.

performance on the HPatches dataset, which indicate a substantial improvement with our modification.

2.4. Depth consistency verification

In addition to semantic segmentation, recent advances in monocular depth prediction also enables a strong depth constraint on feature matching for accurate visual localization. In this section, we propose DCV which effectively identify fallacious matched features associated with low depth consistency. SfM produces a cloud of 3D points with a set of database images, each one of which corresponds to a specific feature point in database image [4]. After feature matching is completed between 2D points in query image and the correctly retrieved database image, the correspondence between the query feature points and 3D points is built. Assuming this is found correctly, the depth estimate of one of the feature points is found by projecting the corresponding 3D point to image plane:

$$P_{img} = K(RP_{wrld} + T), \tag{3}$$

where P_{wrld} is the coordinate of 3D point, P_{img} is the image coordinates, K is the intrinsic matrix, R is the estimated rotation matrix and T is the estimated translation matrix with PnP. With known x and y coordinates of the feature point, the scale of P_{img} can be determined hence its z coordinate, or the *estimated depth value* (EDV). This allows us to check the depth value against the one obtained from a deep network such as the work reported in [33], or the *predicted depth value* (PDV).

For ease of explanation, let us first consider an *ordinary ordinal cost*. Since the scale of the PDV is often unknown, it cannot be compared directly with EDV. One possible solution is to compare their ordinal value. However, the depth values of different keypoints are not evenly spaced in most cases, and this leads to out-of-scale. To overcome this issue, we calculated the *adaptive ordinal cost* (AOC) by:

$$C = abs(D[i] - D[j]), \tag{4}$$



Figure 4: Experiment results showing the identified inconsistent matches: depth prediction in jet-map is on left and matched features on the right, where consistent and inconsistent matches are shown in cyan and red respectively.

where C is the AOC, D is the PDV, and i and j are the ordinal values in the EDVs and the PDVs respectively. Assuming the predicted depth is considerably accurate, the AOC scales well for different value intervals. After AOC is estimated for all feature points, they are divided by their mean to cope with the unknown scale.

The effectiveness of the proposed DCV is shown in Figure 4, where inconsistent matches are clearly identified. Though there are some false detection due to the inevitable inaccuracy in 3D map generation and monocular depth prediction, they are further neglected by comparing the reprojection error before and after being removed. Nevertheless, a significant portion of inconsistent matches are identified which seriously affect the estimation accuracy.

2.5. Pose estimation with weighted-RANSAC

After incorrect matches are removed by SCC and DCV in per query-retrieval pair, an overall set of matches are taken between 2D keypoints in the query image and 3D points corresponding to all the retrieved images, allowing the final PnP pose computation. A standard RANSAC PnP compute a hypothetical pose M with a subset of input matches, and all the other samples are tested by computing reprojection error e_p with the pose. A sample p is accepted as an inlier if the error is below a preset threshold e_t , shown by the following indicator function:

$$T(p, M) = \begin{cases} 1, & e_p < e_t \\ 0, & otherwise. \end{cases} \quad (5)$$

This process is repeated for a number of random samples until enough inliers are found. We again leverage semantic information by the proposed weighted-RANSAC scheme, where the threshold is reduced according to semantic consistency, defined by the new indicator function:

$$weight_{\mu} T(p, M) = \begin{cases} 1 - \left(\frac{e_p}{\mu \cdot e_t}\right)^2, & |e_p| < (\mu \cdot e_t) \\ 0, & otherwise, \end{cases} \quad (6)$$

where μ is the reduction ratio calculated by normalizing SCW that is defined in Eqn. 1.

3. Conclusion

In this paper, we proposed a visual localization pipeline leveraging semantic and depth cues. We propose SCW to remove erroneous image retrieval results, SCC to reduce the number of incorrect image retrieval results based on semantic consistency, and DCV to remove matches that have poor depth consistency. We use the proposed enhanced-R2D2 descriptor and the combination of R2D2 and SuperPoint feature extractor to demonstrate their effectiveness for higher localization accuracy and robustness. Finally, the outliers of pose estimates are removed with clustering and the final pose estimation is performed by a weighted-RANSAC scheme. Extensive experimental results show that our method achieves the state-of-art performance on the benchmark.

References

- [1] Hyon Lim, Sudipta N Sinha, Michael F Cohen, and Matthew Uyttendaele. Real-time image-based 6-dof localization in large-scale environments. In *Proceedings of the IEEE Conference on Computer Vision and Pattern Recognition*, pages 1043–1050. IEEE, 2012.
- [2] Robert O. Castle, Georg Klein, and David W. Murray. Video-rate localization in multiple maps for wearable augmented reality. In *IEEE International Symposium on Wearable Computers*, 2008.
- [3] Wei-Tung Wang, Yi-Leh Wu, Cheng-Yuan Tang, and Maw-Kae Hor. Adaptive density-based spatial clustering of applications with noise (dbscan) according to data. In *International Conference on Machine Learning and Cybernetics*, volume 1, pages 445–451. IEEE, 2015.
- [4] Johannes L Schonberger and Jan-Michael Frahm. Structure-from-motion revisited. In *Proceedings of the IEEE Conference on Computer Vision and Pattern Recognition*, pages 4104–4113, 2016.
- [5] Shimon Ullman. The interpretation of structure from motion. *Proceedings of the Royal Society of London. Series B. Biological Sciences*, 203(1153):405–426, 1979.
- [6] Jorge Fuentes-Pacheco, José Ruiz-Ascencio, and Juan Manuel Rendón-Mancha. Visual simultaneous localization and mapping: a survey. *Artificial Intelligence Review*, 43(1):55–81, 2015.
- [7] Christoffer Valgren and Achim J Lilienthal. Sift, surf & seasons: Appearance-based long-term localization in outdoor environments. *Robotics and Autonomous Systems*, 58(2):149–156, 2010.

- [8] Xiao-Shan Gao, Xiao-Rong Hou, Jianliang Tang, and Hang-Fei Cheng. Complete solution classification for the perspective-three-point problem. *IEEE Transactions on Pattern Analysis and Machine Intelligence*, 25(8):930–943, 2003.
- [9] Pauline C Ng and Steven Henikoff. Sift: Predicting amino acid changes that affect protein function. *Nucleic Acids Research*, 31(13):3812–3814, 2003.
- [10] Jerome Revaud, Philippe Weinzaepfel, César De Souza, Noe Pion, Gabriela Csurka, Yohann Cabon, and Martin Humenberger. R2d2: Repeatable and reliable detector and descriptor. *arXiv preprint arXiv:1906.06195*, 2019.
- [11] Daniel DeTone, Tomasz Malisiewicz, and Andrew Rabinovich. Superpoint: Self-supervised interest point detection and description. In *Proceedings of the IEEE Conference on Computer Vision and Pattern Recognition Workshops*, pages 224–236, 2018.
- [12] Kwang Moo Yi, Eduard Trulls, Vincent Lepetit, and Pascal Fua. Lift: Learned invariant feature transform. In *Proceedings of the European Conference on Computer Vision*, pages 467–483. Springer, 2016.
- [13] Mihai Dusmanu, Ignacio Rocco, Tomas Pajdla, Marc Pollefeys, Josef Sivic, Akihiko Torii, and Torsten Sattler. D2-net: A trainable cnn for joint description and detection of local features. In *Proceedings of the IEEE Conference on Computer Vision and Pattern Recognition*, pages 8092–8101, 2019.
- [14] CAC Mach. Random sample consensus: a paradigm for model fitting with application to image analysis and automated cartography. *Readings in Computer Vision*, pages 726–740, 1981.
- [15] Arnold Irschara, Christopher Zach, Jan-Michael Frahm, and Horst Bischof. From structure-from-motion point clouds to fast location recognition. In *Proceedings of the IEEE Conference on Computer Vision and Pattern Recognition*, pages 2599–2606. IEEE, 2009.
- [16] Hyeonwoo Noh, Andre Araujo, Jack Sim, Tobias Weyand, and Bohyung Han. Large-scale image retrieval with attentive deep local features. In *Proceedings of the IEEE International Conference on Computer Vision*, pages 3456–3465, 2017.
- [17] Albert Gordo, Jon Almazán, Jerome Revaud, and Diane Larlus. Deep image retrieval: Learning global representations for image search. In *Proceedings of the European Conference on Computer Vision*, pages 241–257. Springer, 2016.
- [18] Marvin Teichmann, Andre Araujo, Menglong Zhu, and Jack Sim. Detect-to-retrieve: Efficient regional aggregation for image search. In *Proceedings of the IEEE Conference on Computer Vision and Pattern Recognition*, pages 5109–5118, 2019.
- [19] Relja Arandjelovic, Petr Gronat, Akihiko Torii, Tomas Pajdla, and Josef Sivic. Netvlad: Cnn architecture for weakly supervised place recognition. In *Proceedings of the IEEE Conference on Computer Vision and Pattern Recognition*, pages 5297–5307, 2016.
- [20] Artem Babenko and Victor Lempitsky. Aggregating local deep features for image retrieval. In *Proceedings of the IEEE International Conference on Computer Vision*, pages 1269–1277, 2015.
- [21] Hengshuang Zhao, Jianping Shi, Xiaojuan Qi, Xiaogang Wang, and Jiaya Jia. Pyramid scene parsing network. In *Proceedings of the IEEE Conference on Computer Vision and Pattern Recognition*, pages 2881–2890, 2017.
- [22] Changqian Yu, Jingbo Wang, Chao Peng, Changxin Gao, Gang Yu, and Nong Sang. Bisenet: Bilateral segmentation network for real-time semantic segmentation. In *Proceedings of the European Conference on Computer Vision*, pages 325–341, 2018.
- [23] Liang-Chieh Chen, Yukun Zhu, George Papandreou, Florian Schroff, and Hartwig Adam. Encoder-decoder with atrous separable convolution for semantic image segmentation. In *Proceedings of the European Conference on Computer Vision*, pages 801–818, 2018.
- [24] Mark Everingham, Luc Van Gool, Christopher KI Williams, John Winn, and Andrew Zisserman. The pascal visual object classes (voc) challenge. *International Journal of Computer Vision*, 88(2):303–338, 2010.
- [25] Marius Cordts, Mohamed Omran, Sebastian Ramos, Timo Rehfeld, Markus Enzweiler, Rodrigo Benenson, Uwe Franke, Stefan Roth, and Bernt Schiele. The cityscapes dataset for semantic urban scene understanding. In *Proceedings of the IEEE Conference on Computer Vision and Pattern Recognition*, pages 3213–3223, 2016.
- [26] Tomasz Trzcinski, Mario Christoudias, Vincent Lepetit, and Pascal Fua. Learning image descriptors with the boosting-trick. In *Advances in Neural Information Processing Systems*, pages 269–277, 2012.
- [27] Anastasiia Mishchuk, Dmytro Mishkin, Filip Radenovic, and Jiri Matas. Working hard to know your

- neighbor’s margins: Local descriptor learning loss. In *Advances in Neural Information Processing Systems*, pages 4826–4837, 2017.
- [28] Yuki Ono, Eduard Trulls, Pascal Fua, and Kwang Moo Yi. Lf-net: learning local features from images. In *Advances in Neural Information Processing Systems*, pages 6234–6244, 2018.
- [29] Vassileios Balntas, Karel Lenc, Andrea Vedaldi, and Krystian Mikolajczyk. Hpatches: A benchmark and evaluation of handcrafted and learned local descriptors. In *Proceedings of the IEEE Conference on Computer Vision and Pattern Recognition*, pages 5173–5182, 2017.
- [30] Dmytro Mishkin, Filip Radenovic, and Jiri Matas. Repeatability is not enough: Learning affine regions via discriminability. In *Proceedings of the European Conference on Computer Vision*, pages 284–300, 2018.
- [31] Mohammed E Fathy, Quoc-Huy Tran, M Zeeshan Zia, Paul Vernaza, and Manmohan Chandraker. Hierarchical metric learning and matching for 2d and 3d geometric correspondences. In *Proceedings of the European Conference on Computer Vision*, pages 803–819, 2018.
- [32] Michal Perd’och, Ondrej Chum, and Jiri Matas. Efficient representation of local geometry for large scale object retrieval. In *Proceedings of the IEEE Conference on Computer Vision and Pattern Recognition*, pages 9–16. IEEE, 2009.
- [33] Zhengqi Li and Noah Snavely. Megadepth: Learning single-view depth prediction from internet photos. In *Proceedings of the IEEE Conference on Computer Vision and Pattern Recognition*, pages 2041–2050, 2018.